

**Final Project Report**

**Project title:** Solid State, Surface and Catalytic Studies of Oxides

**DOE Award Number:** DE-FG02-87ER13725

**Project period:** May 21, 1987 – December 14, 2001.

**Principal Investigator:**

Harold H. Kung, Chemical and Biological Engineering Department, Northwestern University,  
Evanston, IL 60208-3120, hkung@northwestern.edu

**Date:** November, 2004

DOE Patent Clearance Granted

MP Dvorscak

Mark P. Dvorscak

(630) 252-2393

E-mail: mark.dvorscak@ch.doe.gov

Office of Intellectual Property Law

DOE Chicago Operations Office

12/28/04  
Date

### **DISCLAIMER**

This report was prepared as an account of work sponsored by an agency of the United States Government. Neither the United States Government nor any agency thereof, nor any of their employees, makes any warranty, express or implied, or assumes any legal liability or responsibility for the accuracy, completeness, or usefulness of any information, apparatus, product, or process disclosed, or represents that its use would not infringe privately owned rights. Reference herein to any specific commercial product, process, or service by trade name, trademark, manufacturer, or otherwise does not necessarily constitute or imply its endorsement, recommendation, or favoring by the United States Government or any agency thereof. The views and opinions of authors expressed herein do not necessarily state or reflect those of the United States Government or any agency thereof.

## **DISCLAIMER**

**Portions of this document may be illegible in electronic image products. Images are produced from the best available original document.**

## Introduction

Oxides are catalytically important materials. They can be used as catalysts or as catalyst supports. Since oxides can possess basic, acidic, and redox properties, they can catalyze a wide variety of reactions, including some well known examples such as aldol condensation (base catalyzed), alkane cracking (acid catalyzed), and selective oxidation (redox catalyzed). Our research conducted in this project focused mostly on the redox properties of the metal cations in the oxides. Two industrially important reactions were investigated. One was the selective oxidative dehydrogenation of light alkanes, and the other was the hydrocarbon reduction of NO<sub>x</sub>. Our emphasis was to elucidate the relationship between the catalytic and the chemical properties of oxides used in these reactions. A summary of progress are presented below.

### 1. Oxidative Dehydrogenation Of Alkanes Over Vanadium Oxides-Based Catalysts

There has been a strong interest to effect oxidative dehydrogenation of light alkanes such as ethane, propane and butane because of their lower cost relative to the alkene counterparts. Ideally, for oxidative dehydrogenation of alkanes, the formation of alkenes is the only reaction (Eq. 1). In practice, however, nonselective oxidation to carbon oxides (Eq. 2) and other products also occurs.



The emphasis of our work was to increase the understanding of the nature of the active sites and factors that determine selectivity for dehydrogenation.

We were first to report that mixed oxides of vanadium and magnesium (V-Mg-O) show high selectivity for oxidative dehydrogenation of alkane [1,2]. By impregnating a solution of ammonium metavanadate onto MgO or Mg(OH)<sub>2</sub> followed by calcination, mixtures of different magnesium vanadates were formed. The formation of various vanadates could be followed using IR spectroscopy and x-ray diffraction. These vanadates include: magnesium orthovanadate (Mg<sub>3</sub>(VO<sub>4</sub>)<sub>2</sub>), magnesium pyrovanadate (Mg<sub>2</sub>V<sub>2</sub>O<sub>7</sub>), and magnesium metavanadate (MgV<sub>2</sub>O<sub>6</sub>). These vanadates have different structures. Especially of interest is the manner with which the VO<sub>4</sub> tetrahedra are linked to other units in the structure. For example, (Mg<sub>3</sub>(VO<sub>4</sub>)<sub>2</sub>) has isolated VO<sub>4</sub> tetrahedra, α-Mg<sub>2</sub>V<sub>2</sub>O<sub>7</sub> is made up of corner-sharing VO<sub>4</sub> tetrahedra that form V<sub>2</sub>O<sub>7</sub> units, and MgV<sub>2</sub>O<sub>6</sub> is made up of metavanadate chains of edge-sharing VO<sub>5</sub> units.

V-Mg-O catalysts of a range of compositions, from low V content to one equivalent to the formation of Mg pyrovanadate (69 wt.% V<sub>2</sub>O<sub>5</sub>) were studied [1,2,3,4,5,6] for the oxidative dehydrogenation of ethane, propane, butane, 2-methylpropane, and cyclohexane. Other vanadium oxide-based catalysts, including rare earth and base metal vanadates [7,8], SiO<sub>2</sub>- [9] and Al<sub>2</sub>O<sub>3</sub>-supported [10] and unsupported V-P-O [11], as well as Cs-modified supported V<sub>2</sub>O<sub>5</sub> [12], and K- modified V-Mg-O [13] were studied. These catalysts were investigated to examine the effect of the atomic structure of the VO<sub>4</sub> units, the reducibility of the cation in the vanadate, and the effect of dispersion and support on the selectivity of the reaction. With few exceptions, the presence of V increases the activity of the catalyst significantly, suggesting that V is chemically involved in the active sites. In fact, these catalysts produced alkene products in pulse

experiments without oxygen present and the product selectivity remained similar to the steady state experiments, implying that proximate source of oxygen is the solid lattice.

Taking the results together, it was found that the selectivity for dehydrogenation depends on the reducibility of the second cation: a less reducible cation results in a more selective catalyst, as shown in Table 1. For supported vanadia, the selectivity depends on the loading. Generally, lower loading catalysts are more selective, which are also less easily reducible. Raman spectroscopic investigations suggest that the  $\text{VO}_x$  structure of highly dispersed  $\text{V}_2\text{O}_x$  on a support resembles those of orthovanadates. Interestingly, the catalytic behavior also depends on the alkane as shown in Table 2. The selectivity depends on the alkane conversion, being lower at higher conversions (Fig. 1). This is expected for a sequential reaction scheme in which the desired product is an intermediate product. From the data such as that shown in Fig. 1, it can be estimated that on a Mg orthovanadate-MgO catalyst, the rate constant for the conversion of propene to carbon oxides is about 4 times greater than the rate constant for the conversion of propane to propene at 500°C [3].

Table 1: A comparison of the selectivity for alkenes over Mg orthovanadate and Mg pyrovanadate.

Alkane	Mg orthovanadate				Mg pyrovanadate			
	Temp (C)	Alkane. conv. %	Select. %	AOS <sup>d</sup>	Temp (C)	Alkane. conv. %	Select. %	AOS <sup>d</sup>
$\text{C}_2\text{H}_6^a$	540	5.2	24	2.1	540	3.2	30	2.1
$\text{C}_3\text{H}_8^c$	541	6.7	64	2.1	505	7.9	61	2.1
$\text{C}_4\text{H}_{10}^c$	540	8.5	65.9 <sup>b</sup>	2.5	500	6.8	31.8 <sup>b</sup>	3.9
i- $\text{C}_4\text{H}_{10}^a$	500	8	64	2.1	502	6.8	25	4.1

- a: The data for Mg orthovanadate were obtained with 40VMgO, which contained Mg orthovanadate and MgO.  
 b: Sum of selectivity to butenes and butadiene.  
 c: Data using samples of relatively pure phases.  
 d: Average oxygen stoichiometry.

Table 2: Correlation between reduction potential of the cation in orthovanadate and selectivity for oxidative dehydrogenation of butane.

Cation	Reduction potential, V	Butane conv. %	Dehydrog. select. %
Mg	-2.40	5.2	62
Nd	-2.30	8.5	62
Sm	-2.30	7.9	59
Zn	-0.76	6.6	41
Cr	-0.42	5.5	17
Eu	-0.35	5.5	41
Ni	-0.26	7.3	18
Cu	+0.32	6.9	4
Fe	+0.77	6.5	17

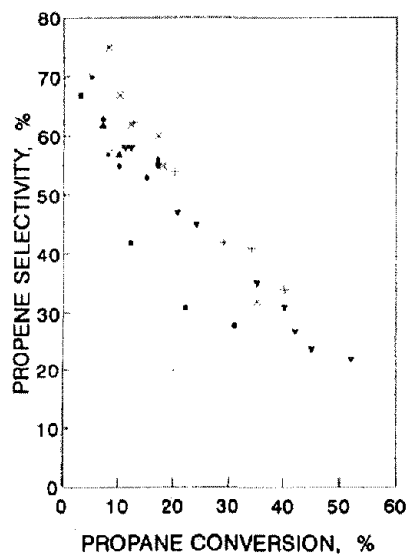
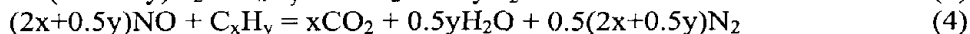


Fig. 1: Illustrative catalytic behavior of V-Mg-O catalysts in the oxidative dehydrogenation of propane.

The mechanism of the reaction was proposed to involve first the abstraction of a H atom from an alkane molecule. This step is likely the rate limiting step, since the overall rate of the alkane oxidation reaction depends on the strength of the C-H bond [4,6]. We have also proposed a selectivity-determining step involving the reaction of an adsorbed alkyl [11]. The number of surface VO<sub>x</sub> units that presumably form the surface active site (that is, that can effectively interact with the adsorbed alkyl and participate in the reaction of one adsorbed molecule) determine the average oxygen stoichiometry. The effective size of such a unit is determined by both the size of the adsorbed hydrocarbon species as well as the rate of reoxidation of the vanadium active center either by lattice diffusion or with oxygen from the gas phase. Thus, for a particular hydrocarbon, catalysts of different compositions but the same effective size of the surface active site (i.e. same average oxygen stoichiometry) would exhibit the same selectivity. Finally, we postulate that the effective size depends on the linkage of VO<sub>4</sub> units in a vanadate structure.

## 2. Alumina-Supported Catalysts for NO Reduction in an Oxidizing Atmosphere

The concern over air quality has resulted in increasingly tightened standards on the permissible emission levels of atmospheric pollutants. In recent years, new standards for light and heavy duty diesel engine exhausts have been promulgated. Meeting these new standards has posed significant challenges for the engine and catalyst manufacturers. The lean-burn operation of these engines results in an exhaust that contains a much higher concentration of oxygen and lower concentration of reductants (hydrocarbon and CO) than in the exhaust of a stoichiometric gasoline engine. Consequently, the highly-developed three-way catalysts used for gasoline engine exhaust are not effective in removing NO<sub>x</sub> from the diesel exhaust; the reductant are consumed by combustion mostly (Eq. 3) instead of by reaction with NO<sub>x</sub> to form N<sub>2</sub> (Eq. 4). New catalysts are needed that can selectively catalyze the reaction between NO and a reductant, which is preferably a hydrocarbon or its derivative, without catalyzing its combustion. This type of reactions is generally known as lean NO<sub>x</sub> catalysis.



The most heavily investigated catalysts for the lean-burn engines are based on zeolites, particularly the MFI type. Cu-ZSM-5 was the first reported and most studied catalyst that demonstrates a high selectivity for NO<sub>x</sub> reduction with small hydrocarbons [14,15], and many other ion-exchanged MFI catalysts have since been studied. However, it was soon discovered that these catalysts suffer from structural degradation after prolonged exposure to the reaction mixture, making it doubtful that they can meet the durability requirement for a commercial product.

We were one of the first few who demonstrated conclusively that alumina-supported catalysts can be quite effective for this reaction. The early results of Iwamoto suggested that alumina-supported catalysts are much inferior to the MFI-supported ones [16]. However, we and other later showed that the preparation, pretreatment, and loading of the catalyst can have significant effects on the effectiveness of alumina-based catalysts in NO<sub>x</sub> reduction. While it is

still generally true that MFI-supported catalysts of the same metal is more active at lower temperatures than an alumina-supported ones, the latter is equally selective for the reaction at somewhat higher temperatures.

*$\gamma$ -Alumina as a lean NO<sub>x</sub> reduction catalyst*

As a catalyst,  $\gamma$ -alumina (whence simply referred to as alumina) has a very low activity at temperatures below around 400°C for the reduction of NO using hydrocarbons in a typical synthetic lean exhaust gas mixture (e.g., 5-10% O<sub>2</sub>, 2-10% H<sub>2</sub>O, 0.1% NO, and 0.1% propene). Figure 2 shows some typical results [17]. Curves A and B show the N<sub>2</sub> yield (%NO in the feed converted to N<sub>2</sub>) as a function of temperature for two different experiments. In the experiment with a higher space velocity and oxygen and water partial pressures (curve A), the NO yield increased steadily with increasing temperature, reaching a maximum at around 600°C. The hydrocarbon conversion paralleled this trend, being low below 450°C, but rose rapidly above 500°C, reaching close to 100% above 550°C. For the experiment with a slower space velocity, the N<sub>2</sub> yield increased steadily with increasing temperature below about 500°C. At that temperature, sustained oscillations in both the N<sub>2</sub> yield and hydrocarbon conversion were observed. The oscillation could be observed within a temperature window of about 10°C. Within this window, the period and the oscillation amplitude pattern are quite sensitively dependent on the temperature [18]. Such oscillation was also observed by others [19].

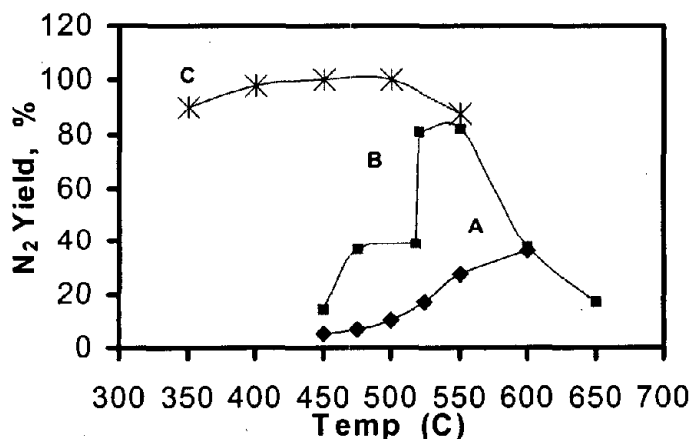


Figure 2. N<sub>2</sub> yield in the reduction of NO or NO<sub>2</sub> over  $\gamma$ -Al<sub>2</sub>O<sub>3</sub>. Curve A (♦): 0.2 g catalyst, 200 mL/min of 0.1%NO, 0.1% propene, 15% O<sub>2</sub>, 10% H<sub>2</sub>O, balance He; curve B (■): 0.25 g catalyst, 100 mL/min of 0.1% NO, 0.1% propene, 6% O<sub>2</sub>, balance He; curve C (\*): 0.25 g catalyst, 100mL/min of 0.1% NO<sub>2</sub>, 0.1% propene, 5% O<sub>2</sub>, balance He.

Although alumina alone can utilize the hydrocarbon reductant with a high efficiency, the temperature required for a substantial activity is too high for practical treatment of diesel engine exhausts. Alumina is much more active in the reduction of  $\text{NO}_2$  with hydrocarbon than in the reduction of  $\text{NO}$ , as shown by curve C in Fig. 1. Significant  $\text{NO}_2$  conversion to  $\text{N}_2$  was observed above  $300^\circ\text{C}$ .  $\text{NO}_2$  is a much more reactive oxidant than  $\text{NO}$ , and it has been shown that exposure of alumina to  $\text{NO}_2$  results in the formation of adsorbed  $\text{NO}_y$  species readily that can react with hydrocarbon [20]. Thus, it may be concluded that activation of hydrocarbon is a slow step on alumina, and higher activities can be obtained by using more reactive reductants. Indeed, under otherwise identical conditions, the reaction temperature necessary for substantial  $\text{NO}_x$  reduction increases as: methanol  $\approx$  ethanol  $<$  2-propanol  $<$  propene  $<$  propane [21]. That is, the more "activated" or oxidized is the hydrocarbon, the easier is its reaction with  $\text{NO}_x$ . This is a consequence of the poor oxidation activity of alumina, not only for hydrocarbons, but also for the oxidation of  $\text{NO}$  to  $\text{NO}_2$  [22,23].

#### *$\gamma$ -Alumina-Supported Catalysts*

The activity of an alumina catalyst can be increased substantially by adding another component. Various metals and oxides have been reported to be effective, including Au [24,25], Ag [17,26],  $\text{CoO}_x$  [27,28],  $\text{SnO}_2$  [29,30], and Pt [31,32]. Alumina-supported Pt has the highest activity at low temperatures, but  $\text{N}_2\text{O}$  is a significant product, especially at low temperatures high hydrocarbon conversion. For all of these catalysts, the catalytic performance has an apparent dependence on the loading of the supported phase. For example, the selectivity for hydrocarbon reduction of  $\text{NO}$  versus hydrocarbon combustion is much higher for a low-loading Ag/ $\text{Al}_2\text{O}_3$  than a high loading one [17,26]. Similarly, a low-loading  $\text{CoO}_x/\text{Al}_2\text{O}_3$  catalyst is much more effective than a high loading sample (Fig. 3) [28].

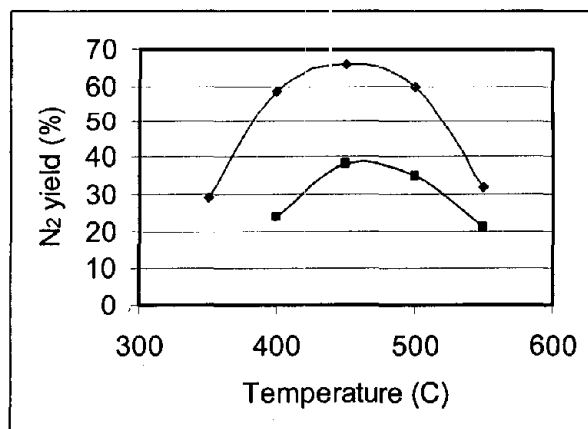


Figure 3: Reduction of  $\text{NO}$  over  $\text{CoO}_x/\gamma\text{-Al}_2\text{O}_3$ . (♦) 0.5 g 2 wt.% Co, pretreated at  $550^\circ\text{C}$ , 100 mL/min of 0.1%  $\text{NO}$ , 0.1% propene, 5%  $\text{O}_2$ , 1.7%  $\text{H}_2\text{O}$ , balance He; (■): 0.5 g 5 wt.% Co, pretreated at  $550^\circ\text{C}$ , same feed.

The reasons for the dependence on loading differ for different materials. For Ag/Al<sub>2</sub>O<sub>3</sub>, the smaller Ag particles in low-loading samples are more difficult to be reduced to metallic Ag than large Ag particles. The ionic Ag is believed to be much more effective for NO<sub>x</sub> reduction, whereas metallic Ag particles are more active for combustion, and produces a substantial amount of N<sub>2</sub>O. For CoO<sub>x</sub>/Al<sub>2</sub>O<sub>3</sub>, highly dispersed CoO<sub>x</sub> that interacts strongly with Al<sub>2</sub>O<sub>3</sub> is much less active for hydrocarbon combustion than Co<sub>3</sub>O<sub>4</sub> that exists in high-loading samples. In the case of Pt/Al<sub>2</sub>O<sub>3</sub>, the activity of Pt is a strong function of dispersion. The activities for NO reduction (to N<sub>2</sub> and N<sub>2</sub>O) and the corresponding hydrocarbon oxidation, and oxidation of NO to NO<sub>2</sub> all decrease with increasing Pt dispersion [33]. Interestingly, Pt dispersion has much less effect on the ratio of N<sub>2</sub> to N<sub>2</sub>O products [32,33].

Contrary to these examples, the effect of dispersion of SnO<sub>2</sub> in SnO<sub>2</sub>/Al<sub>2</sub>O<sub>3</sub> shows a somewhat different behavior. At low loadings, increasing the SnO<sub>2</sub> content increases the NO reduction activity, which is expected if SnO<sub>2</sub> is the active phase. However, a maximum NO reduction activity is attained at a loading of 5-10 wt.% Sn. Further increase in loading decreases the activity [29] (Fig. 4). X-ray diffraction of these samples shows that SnO<sub>2</sub> first exists in an X-ray amorphous form at low loadings, and crystalline SnO<sub>2</sub> are formed at higher loadings. The presence of at least these two forms of SnO<sub>2</sub> is consistent with the temperature programmed reduction results (Fig. 5), which show only a broad reduction peak for low-loading samples and the appearance of a much sharper, high-temperature peak for high loading samples. The features can be assigned to amorphous and crystalline SnO<sub>2</sub>, respectively. Since the surface area of crystalline SnO<sub>2</sub> is small, the observed catalytic behavior would be mostly due to amorphous SnO<sub>2</sub>, the amount of which would reach a maximum after a certain loading.

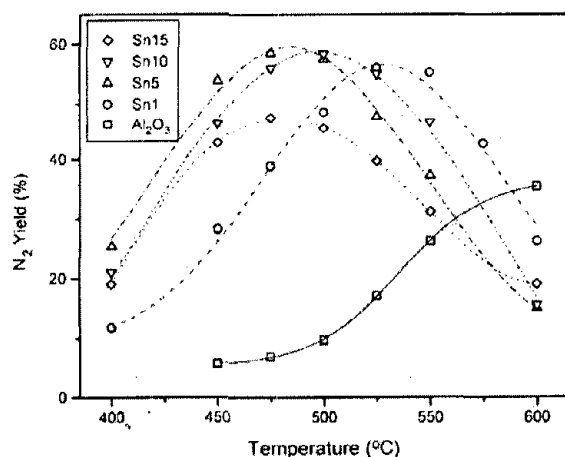


Figure 4: Reduction of NO over SnO<sub>2</sub>/γ-Al<sub>2</sub>O<sub>3</sub> of different Sn loadings, ranging from 0 to 15 wt.% Sn. 0.1%NO, 0.1% propene, 15% O<sub>2</sub>, 10% H<sub>2</sub>O, balance He, space velocity 30,000 h<sup>-1</sup>.

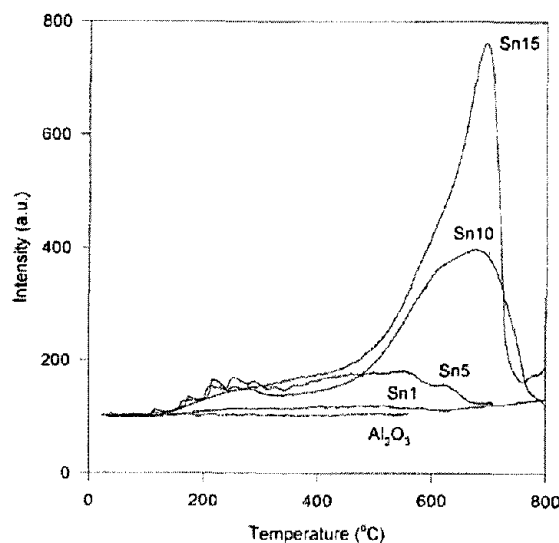


Figure 5: H<sub>2</sub>-Temperature programmed reduction of SnO<sub>2</sub>/Al<sub>2</sub>O<sub>3</sub> catalysts samples in Fig. 4.

However, the behavior of these catalysts seems to be more complicated. If amorphous SnO<sub>2</sub> is the active phase that contributes to most of the observed activity, then why do the higher loading samples not only have lower activity for NO reduction, but also have lower selectivity for this reaction compared with hydrocarbon combustion (as indicated by lower maximum N<sub>2</sub> yield)? The attempt to answer this question led to the observations described below.

#### *Bifunctional SnO<sub>2</sub>/Al<sub>2</sub>O<sub>3</sub>*

If SnO<sub>2</sub> is the only active phase, then the conversion and product distributions should be the same as long as there is the same amount of amorphous SnO<sub>2</sub> in a reactor (under otherwise identical reaction conditions). That is, one would expect that the observations from an experiment using 0.2 g of a sample containing 1 wt.% Sn would be the same as those using 0.04 g of another sample containing 5 wt.% Sn, since the SnO<sub>2</sub> in both samples are mostly in the amorphous form (Fig. 5), and the 5 wt.% sample is approximately five times more active than the 1 wt.% sample (Fig. 4). However, this is not the case, as shown in Fig. 6 [34]. Under the conditions used, 0.04 g of the 5 wt.% sample showed very low NO reduction activity compared with 0.2 g 1 wt.% sample, although their hydrocarbon conversion activities were quite similar. One major difference between these two experiments is the amount of Al<sub>2</sub>O<sub>3</sub> in the reactor. When 0.16 g of Al<sub>2</sub>O<sub>3</sub> was added to 0.04 g of the 5 wt.% sample to make a physical mixture of the same composition as the 1 wt.% sample, a substantial increase in NO reduction activity was observed (Fig. 6, curve C).

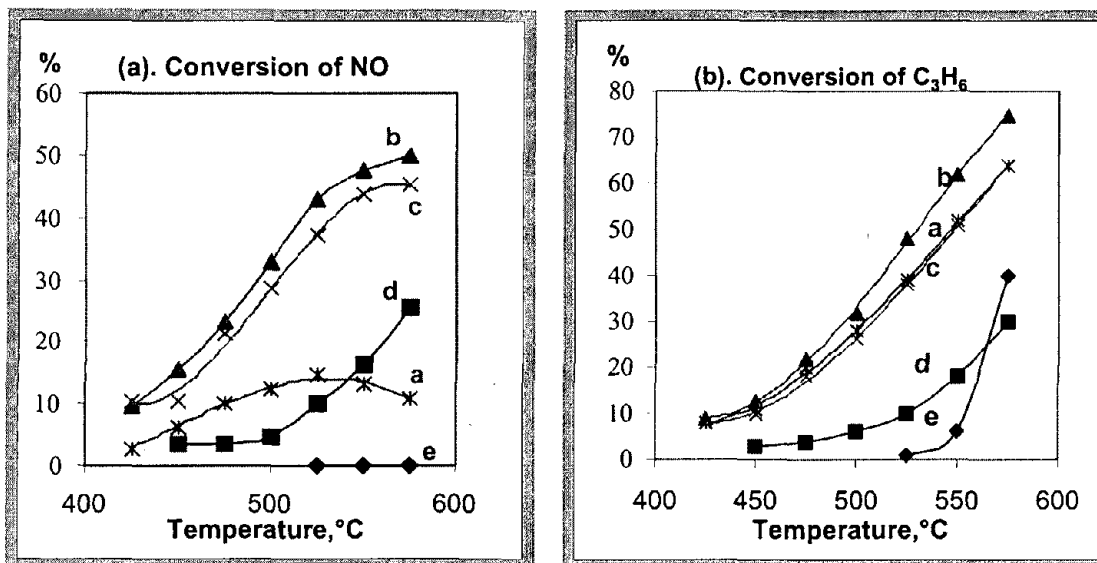


Figure 6: Conversion of (a) NO and (b) propene. Curve a: 0.04 g SnO<sub>2</sub>/Al<sub>2</sub>O<sub>3</sub> containing 5 wt.% Sn; curve b: 0.2 g SnO<sub>2</sub>/Al<sub>2</sub>O<sub>3</sub> containing 1 wt.% Sn; curve c: physical mixture of 0.04 g 5wt.% Sn sample with 0.16 g Al<sub>2</sub>O<sub>3</sub>; Curve d: 0.16 g Al<sub>2</sub>O<sub>3</sub>; curve e: blank reactor. 15% O<sub>2</sub>, 10% H<sub>2</sub>O, 0.1% NO, 0.11% propene, balance He.

The results of Fig. 6 indicate that SnO<sub>2</sub>/Al<sub>2</sub>O<sub>3</sub> is a bifunctional catalyst; both SnO<sub>2</sub> and Al<sub>2</sub>O<sub>3</sub> are necessary for effective NO reduction. In order to further test this, the catalytic activity of a SnO<sub>2</sub>/SiO<sub>2</sub> containing 5 wt.% Sn was tested. The results, as illustrated in Table 3, show that in the absence of Al<sub>2</sub>O<sub>3</sub>, SnO<sub>2</sub> catalyzes the oxidation of propene primarily to acrolein, with the formation of some acetaldehyde also. However, little NO reduction takes place. Furthermore, the catalyst is not active for NO oxidation to NO<sub>2</sub>, as the NO<sub>2</sub> concentration at the reactor exit was the same as the background level. These results imply that on SnO<sub>2</sub>/Al<sub>2</sub>O<sub>3</sub>, the function of SnO<sub>2</sub> is to oxidize propene to acrolein. The acrolein formed is transported in the gas phase to alumina, where reduction of NO occurs.

Table 3: Product concentrations in reactor exit. Reaction condition: 15% O<sub>2</sub>, 10% H<sub>2</sub>O, 0.1% NO, 0.11% propene, balance He, 475°C.

Sample	Product concentration, ppm				
	N <sub>2</sub>	CO <sub>x</sub>	acetaldehyde	acrolein	NO <sub>2</sub>
5 wt.% Sn/SiO <sub>2</sub> (0.1 g)	0	318	37	109	41
Al <sub>2</sub> O <sub>3</sub> (0.1 g)	10	68	0	0	41
5%Sn/SiO <sub>2</sub> + Al <sub>2</sub> O <sub>3</sub>	80	829	20	0	Not determined
Blank	0	0	0	0	40

This assignment of functions to the two components in SnO<sub>2</sub>/Al<sub>2</sub>O<sub>3</sub> is substantiated by the results of a two-bed experiment shown in Fig. 7 [34]. In this experiment, a bed of SnO<sub>2</sub>/SiO<sub>2</sub> and a bed of Al<sub>2</sub>O<sub>3</sub> were placed in two separate reactors, as schematically shown in the figure. The flow of the feed stream could be configured to enter either reactor first. When the feed configuration was such that the SnO<sub>2</sub>/SiO<sub>2</sub> bed was upstream of the Al<sub>2</sub>O<sub>3</sub> bed, substantial NO reduction occurred. However, when the direction of the gas flow was reversed, such that the Al<sub>2</sub>O<sub>3</sub> bed was upstream of the SnO<sub>2</sub>/SiO<sub>2</sub> bed, much less NO reduction took place, although the hydrocarbon conversion remained about the same. Thus, hydrocarbon conversion on SnO<sub>2</sub> precedes NO reduction on Al<sub>2</sub>O<sub>3</sub>.

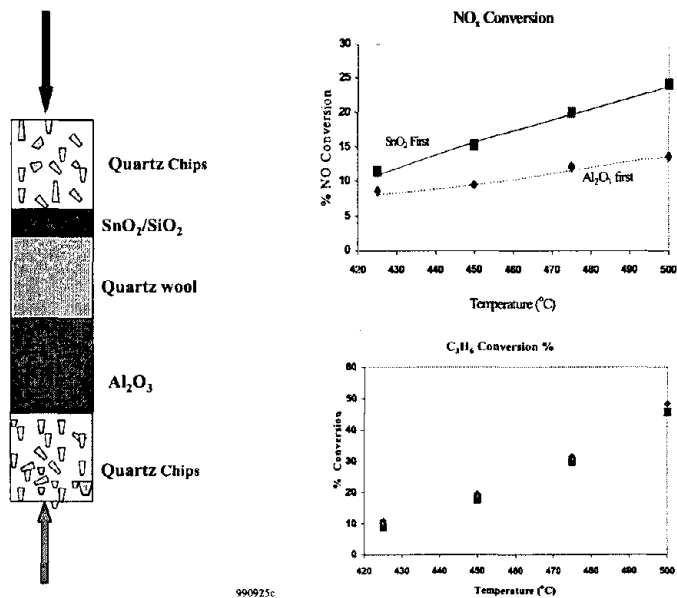
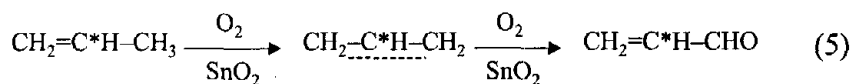


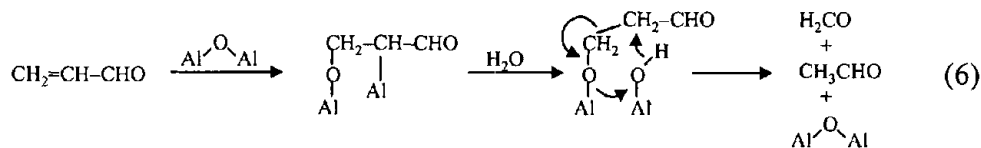
Figure 7: NO and C<sub>3</sub>H<sub>6</sub> conversion for experiments using separated beds of SnO<sub>2</sub>/SiO<sub>2</sub> and Al<sub>2</sub>O<sub>3</sub>. Experimental conditions same as Fig. 6.



The propene oxidation function of SnO<sub>2</sub> was investigated separately. It was found that the oxidation reaction makes use of oxygen as the oxidant, since whether NO is present in the feed has little effect. If the propene molecule is labeled at the center carbon with <sup>13</sup>C, 2-<sup>13</sup>C-labelled acrolein was formed exclusively. Thus, the oxidation reaction proceeds via a symmetric π-allyl intermediate commonly observed in selective oxidation of propene (Eq. 5)

The subsequent steps of the reaction take place on alumina. When the reaction of acrolein was studied over alumina, it was found that acrolein reacts rapidly to form acetaldehyde

and formaldehyde. Interestingly, no NO reduction to N<sub>2</sub> occurred in this step. The presence of water is important for this step, as little acetaldehyde was detected without water in the feed stream. In addition, the N<sub>2</sub> yield dropped to about 60% of the yield with water. The formation of acetaldehyde from acrolein is by cleavage of the C=C bond, since 2-<sup>13</sup>C-labeled acrolein produces mostly <sup>13</sup>CH<sub>3</sub>CHO. Thus, this step is the reverse of an aldol condensation reaction (Eq. 6). We postulate that a bridging Al-O-Al is the catalytic site.



The reaction of acetaldehyde on alumina is rather slow, of the order of ten times slower than acrolein, and the products are mostly CO (about 80%) and CO<sub>2</sub>. Some small amounts of HCN are also formed. At the same time, NO is reduced to N<sub>2</sub>.

The bifunctional nature of SnO<sub>2</sub>/Al<sub>2</sub>O<sub>3</sub> explains the dependence of the NO reduction efficiency on the SnO<sub>2</sub> loading. At very low SnO<sub>2</sub> loadings, the oxidation of propene to acrolein is limiting the overall reaction rate, and the catalytic activity increases with increasing SnO<sub>2</sub> loading. When the SnO<sub>2</sub> loading is high, the overall reaction rate is limited by the rate of reaction of acetaldehyde on Al<sub>2</sub>O<sub>3</sub>. Then, the reaction rate decreases with increasing SnO<sub>2</sub> loading, since the surface area of exposed Al<sub>2</sub>O<sub>3</sub> decreases.

#### *Other bifunctional catalysts*

Ag/Al<sub>2</sub>O<sub>3</sub> is also a bifunctional catalyst. As mentioned earlier, the NO reduction efficiency of this catalyst depends on the Ag loading, and samples of low loadings are more effective than high loadings. Table 4 shows some typical data for a 6 wt.% Ag/Al<sub>2</sub>O<sub>3</sub> sample [17]. Even at 100% propene conversion, the reduction of NO to N<sub>2</sub> was only 15%. There was also a substantial amount of N<sub>2</sub>O formed. The yield of N<sub>2</sub> was substantially increased by using a physical mixture of 6 wt.% Ag/Al<sub>2</sub>O<sub>3</sub> and Al<sub>2</sub>O<sub>3</sub>, higher than the sum of the yields from the individual components. The enhancement in reactivity was not observed when the Al<sub>2</sub>O<sub>3</sub> was replaced with SiO<sub>2</sub> in the physical mixture. Interestingly, for this system, the synergistic effect between components was absent when the 6 wt.% Ag/Al<sub>2</sub>O<sub>3</sub> and Al<sub>2</sub>O<sub>3</sub> catalysts were separated physically by quartz wool. This suggests that the reaction intermediate, which is formed on Ag and transported to Al<sub>2</sub>O<sub>3</sub> for further reaction to reduce NO, is quite reactive. That this synergistic effect is not due to silver migration from the 6 wt.% Ag/Al<sub>2</sub>O<sub>3</sub> catalyst to Al<sub>2</sub>O<sub>3</sub> was shown by recovery of the original catalytic properties when the physical mixture was separated into its individual components after reaction by sieving.

Table 4: NO Reduction over Ag/Al<sub>2</sub>O<sub>3</sub>. Reaction conditions: 0.1% NO, 0.1% propene, 6% O<sub>2</sub>, balance He, 673 K.

Catalyst	NO conv. to N <sub>2</sub> (%)	C <sub>3</sub> H <sub>6</sub> conv. %
0.25 g 6 wt.% Ag/Al <sub>2</sub> O <sub>3</sub>	16	100
0.022 g 6 wt.% Ag/Al <sub>2</sub> O <sub>3</sub>	7	72
0.25 g Al <sub>2</sub> O <sub>3</sub>	11	8
0.022 g 6 % Ag/Al <sub>2</sub> O <sub>3</sub> + 0.23 g Al <sub>2</sub> O <sub>3</sub>	42	77
0.022 g 6 % Ag/Al <sub>2</sub> O <sub>3</sub> + 0.23 g SiO <sub>2</sub>	7	68

The bifunctional nature of supported alumina catalysts has also been observed on other catalysts. Pt/SiO<sub>2</sub> is inactive for the selective reduction of NO by C<sub>3</sub>H<sub>8</sub>, whereas Pt/Al<sub>2</sub>O<sub>3</sub> is a relatively good catalyst. Inaba, et al. observed that the total NO<sub>x</sub> conversions over a physical mixture of 80-100 mesh Pt/SiO<sub>2</sub> and Al<sub>2</sub>O<sub>3</sub> approach that of Pt/Al<sub>2</sub>O<sub>3</sub> [35]. Although Pt catalyzes NO oxidation effectively, at temperatures where significant synergistic effects are present (300 and 350 °C), the role of NO<sub>2</sub> should be minimal since, at these temperatures, the formation of N<sub>2</sub> from NO<sub>2</sub> reduction over Al<sub>2</sub>O<sub>3</sub> is negligible. Thus, the synergistic effect is due to the formation of some reactive intermediates on Pt, other than NO<sub>2</sub>, which can effectively reduce NO on Al<sub>2</sub>O<sub>3</sub>.

#### Publications resulted from this work

1. "Selective Oxidative Dehydrogenation of Butane over V-Mg-O Catalysts", M.A. Chaar, D. Patel, M.C. Kung, and H.H. Kung, *J. Catal.*, **105**, 483 (1987).
2. "Selective Oxidative Dehydrogenation of Propane over V-Mg-O Catalysts," M.A. Chaar, D. Patel, and H.H. Kung, *J. Catal.*, **109**, 463 (1988).
3. "Selective Oxidative Dehydrogenation of Alkanes over Mg Vanadates," D. Patel, M.C. Kung, and H.H. Kung, *Proc. 9th Intern. Congr. Catal.*, **4**, 1554 (1988).
4. "Selective Oxidative Dehydrogenation of Light Alkanes over Vanadate Catalysts," M. Kung, K. Nguyen, D. Patel, and H. Kung, in *Catalysis of Organic Reactions*, ed. D.W. Blackburn, Marcel Dekker Publ., New York, 1990, p.289.
5. "Generation of Gaseous Radicals by a V-Mg-O Catalyst During Oxidative Dehydrogenation of Propane," K. Nguyen, and H. Kung, *J. Catal.*, **122**, 415 (1990).
6. "Oxidative Dehydrogenation of Butane over Orthovanadates," D. Patel, P. J. Andersen, and H. Kung, *J. Catal.*, **125**, 130 (1990).
7. "Analysis of the Postcatalytic Homogeneous Reactions During Oxidative Dehydrogenation of Propane over a V-Mg-O Catalyst," K. Nguyen, and H. Kung, *Ind. & Eng. Chem. Res.*, **30**, 352 (1991).
8. "Oxidative Dehydrogenation of Cyclohexane over Vanadate Catalysts," M.C. Kung, and H.H. Kung, *J. Catal.*, **128**, 287 (1991).
9. "Heterogeneous-Homogeneous reaction Pathways in Oxidative Dehydrogenation of Propane," K.

- Nguyen, and H. Kung, in "Novel Methods of Producing Ethylene, Other Olefins, and Aromatics," ed. L.F. Albright, B.L. Crynes, and S. Nowak, Marcel Dekker, Inc., New York, 1992, p.285.
10. "Deactivation of Methanol Synthesis Catalysts - a Review," H.H. Kung, *Catalysis Today*, **11**, 443 (1992).
  11. "The Effect of Oxide Structure and Cation Reduction Potential of Vanadates on the Selective Oxidative Dehydrogenation of Butane and Propane," O.S. Owen, M.C. Kung, and H.H. Kung, *Catal. Lett.*, **12**, 45 (1992).
  12. "Kinetic Analysis of a Generalized Catalytic Selective Oxidation Reaction," H.H. Kung, *J. Catal.*, **134**, 691 (1992).
  13. "The Effect of Potassium in the Preparation of Mg Orthovanadate and Pyrovanadate on the Oxidative Dehydrogenation of Propane and Butane," M.C. Kung, and H.H. Kung, *J. Catal.*, **134**, 668 (1992).
  14. "A Kinetic Model of the Epoxidation of Ethylene," H.H. Kung, *Chem. Eng. Commun.*, **118**, 17 (1992).
  15. "Effects of Loading and Cesium Modifier on Silica-supported Vanadia in Oxidative Dehydrogenation of Butane," L. Owens, and H.H. Kung, *Prep. Amer. Chem. Soc. Div. Petrol. Chem.*, **37**, 1194 (1992).
  16. "A Comparison of  $Mg_3(VO_4)_2$ ,  $Mg_2V_2O_7$ , and  $(VO)_2P_2O_7$  in Alkane Oxidation," P.M. Michalakos, M.C. Kung, I. Jahan, and H.H. Kung, *Prep. Amer. Chem. Soc. Div. Petrol. Chem.*, **37**, 1201 (1992).
  17. "Selectivity Patterns in Alkane Oxidation over  $Mg_3(VO_4)_2$ ,  $Mg_2V_2O_7$ , and  $(VO)_2P_2O_7$ ," P.M. Michalakos, M.C. Kung, I. Jahan, and H.H. Kung, *J. Catal.*, **140**, 226 (1993).
  18. "The Effect of Cation Reducibility on the Oxidative Dehydrogenation of Butane in Orthovanadates," Ozie S. Owen and Harold H. Kung, *J. Molec. Catal.*, **79**, 265 (1993).
  19. "Factors that Determine Selectivity for Dehydrogenation in the Oxidation of Light Alkanes," H.H. Kung, P. Michalakos, L. Owens, M. Kung, P. Andersen, O. Owen, and I. Jahan, in "Catalytic Selective Oxidation," ACS Symposium series 523, Ed. S.T. Oyama and J. W. Hightower, 1993, p. 389.
  20. "The Effect of Loading of Vanadia on Silica in the Oxidation of Butane," L. Owens, and H.H. Kung, *J. Catal.*, **144**, 202 (1993).
  21. "Butane and Pentane Oxidation on  $V_2O_5/SiO_2$  Catalysts," K.E. Birkeland, W.D. Harding, L. Owens, and H.H. Kung, *Prepr. ACS Div. Petrol. Chem.*, **38**, 880 (1993).
  22. "Oxidative Dehydrogenation of Light ( $C_2-C_6$ ) Alkanes," H. H. Kung, *Adv. Catal.*, **40**, 1 (1994).
  23. "Effect of Cesium modification of Silica-Supported Vanadium Oxide Catalysts in Butane Oxidation," L. Owens, and H.H. Kung, *J. Catal.* **148**, 587 (1994).
  24. " $NO_x$  Reduction by Propene in an Oxidizing Atmosphere over Cu-ZrO<sub>2</sub>," M.C. Kung, K.A. Bethke, and H.H. Kung, *Prepr. ACS Div. Petrol. Chem.*, **39**, 154 (1994).
  25. "Selective Oxidation of Butane on Phosphorus-Modified Silica Supported Vanadia Catalysts," W.D. Harding, K.E. Birkeland, and H.H. Kung, *Catal. Lett.*, **28**, 1 (1994).
  26. "Catalytic Reduction of Nitric Oxide with Propene over Coprecipitated Cu-ZrO<sub>2</sub> and Cu-Ga<sub>2</sub>O<sub>3</sub>," M. Kung,

- K. Bethke, D. Alt, B. Yang, and H. Kung, in *Reduction of Nitrogen Oxide Emission*, ACS Symposium Series No. 587, U. Ozkan, S. Agrawal, and G. Marcelin ed., 1995, p.96.
27. "The Role of NO<sub>2</sub> in the Reduction of NO by Hydrocarbon over Cu-ZrO<sub>2</sub> and Cu-ZSM-5 Catalysts," K.A. Bethke, C. Li, M.C. Kung, B. Yang, and H. H. Kung, *Catal. Lett.* **31**, 287 (1995).
  28. "Detection of Surface CN and NCO Species as Reaction Intermediates in Catalytic Lean NO<sub>x</sub> Reduction," C. Li, K.A. Bethke, H.H. Kung, and M.C. Kung, *J. Chem. Soc. Chem. Commun.*, 813 (1995).
  29. "Selective Oxidation of Pentane over Al<sub>2</sub>O<sub>3</sub>- and SiO<sub>2</sub>-Supported Vanadia Catalysts," P.M. Michalakos, K. Birkeland, and H.H. Kung, *J. Catal.*, **158**, 349 (1996).
  30. "Metal Oxide Catalysts for Lean NO<sub>x</sub> Reduction." K.A. Bethke, M.C. Kung, B. Yang, M. Shah, D. Alt, C. Li, and H.H. Kung, *Catalysis Today*, **26**, 169 (1995).
  31. "Lean NO<sub>x</sub> Reduction over Au/γ-Al<sub>2</sub>O<sub>3</sub>," M.C. Kung, J.-H. Lee, J. Brooks, and H.H. Kung, *Prepr. Pap. Amer. Chem. Soc., Div. Fuel Chem.*, **40**, 1073 (1995).
  32. "Catalytic Lean NO<sub>x</sub> Reduction over Mixed Metal Oxides, and its Common Features with Selective Oxidation of Alkanes," H.H. Kung and M.C. Kung, *Catal. Today*, **30**, 5 (1996).
  33. "Deactivation of Cu/ZSM-5 Catalysts for Lean NO<sub>x</sub> Reduction - Characterization of Changes of Cu States and Zeolite Support," J.Y. Yan, G.-D. Lei, W.M.H. Sachtler, and H.H. Kung, *J. Catal.*, **161**, 43 (1996).
  34. "Preparation of Oxide Catalysts and Catalyst Supports - a Review of Recent Advances," H.H. Kung and E.I. Ko, *Chem. Eng. J.*, **64**, 203 (1996).
  35. "Effect of Cu Loading and Addition of Modifiers on the Stability of Cu/ZSM-5 in Lean NO<sub>x</sub> Reduction Catalysis," J.Y. Yan, W.M.H. Sachtler, and H.H. Kung, *Catal. Today*, **33**, 279 (1997).
  36. "Understanding the Surface Chemistry of (VO)<sub>2</sub>P<sub>2</sub>O<sub>7</sub>; Butane Oxidation on Silica-Supported Vanadium-Phosphorus Oxides," *Prepr. - Amer. Chem. Soc., Div. Pet. Chem.*, **41**, 197 (1996).
  37. "Selective Reduction of NO<sub>x</sub> by Propene over Au/γ-Al<sub>2</sub>O<sub>3</sub> Catalysts," M.C. Kung, J.-H. Lee, A. Chu-Kung, and H.H. Kung, *Proc. 11th Intern. Cong. Catal.*, J.W. Hightower, W.N. Delgass, E. Iglesia, and A.T. Bell, ed., 1996, p.701.
  38. "Effect of SiO<sub>2</sub> Support on the Preparation of VPO Catalysts for n-Butane Oxidation," J.M.C. Bueno, G.K. Bethke, M.C. Kung, and H.H. Kung, *Proc. XV Simposio Iberoamericano de Catalisis*, Cordoba, Argentina, Sept. 16-20, 1996.
  39. "Supported VPO Catalysts for Selective Oxidation of Butane. II: Characterization of VPO/SiO<sub>2</sub> Catalysts," K.E. Birkeland, S. Babitz, G. Bethke, H.H. Kung, G.W. Coulston, and S.R. Bare, *J. Phys. Chem.B*, **101**, 6895 (1997).
  40. "Oxidative Dehydrogenation of Alkanes over Vanadium-Magnesium-Oxides," H.H. Kung, and M.C. Kung, *Appl. Catal. A*, **157**, 105 (1997).
  41. "The Kinetic Significance of V(5+) in n-Butane Oxidation catalyzed by Vanadium Phosphate," G.W. Coulston, S.R. Bare, H.H. Kung, K. Birkeland, G. Bethke, R. Harlow, and P.L. Lee, *Science*, **275**, 191

(1997).

42. "Supported Ag Catalysts for the Lean Reduction of NO with C<sub>3</sub>H<sub>6</sub>," K.A. Bethke and H.H. Kung, *J. Catal.* **172**, 93 (1997).
43. "Effect of Nature of Silica and P/V Ratio on Silica-supported VPO Catalysts for the Selective Oxidation of Butane," J.M.C. Bueno, G.K. Bethke, M.C. Kung, and H.H. Kung, *Proc. 9th Brazilian Congress on Catalysis*, **2**, 401 (1997).
44. "Alkane Oxidation over Bulk and Silica-Supported VO(H<sub>2</sub>PO<sub>4</sub>)<sub>2</sub>-Derived Catalysts," G.K. Bethke, D. Wang, J.M.C. Bueno, M.C. Kung and H.H. Kung, *Proc. 3rd World Congress on Oxidation Catalysis, Studies Surf. Sci. Catal.*, ed. R.K. Grasselli, S.T. Oyama, A.M. Gaffney, and J.E. Lyons, Elsevier Sci. Publ., vol. 110, p. 453 (1997).
45. "Catalysis for Lean NO<sub>x</sub> Reduction: Structure-Property Relationship," M.C. Kung, K.A. Bethke, J. Yan, J.-H. Lee, and H.H. Kung, *Appl. Surf. Sci.*, **121/122**, 261 (1997).
46. "Co/Al<sub>2</sub>O<sub>3</sub> Lean NO<sub>x</sub> Reduction Catalyst," J.-Y. Yan, M.C. Kung, W.M.H. Sachtler, and H.H. Kung, *J. Catal.*, **172**, 178 (1997).
47. "Reduction of NO<sub>x</sub> in an Oxidizing Atmosphere with Hydrocarbons," H.H. Kung and M.C. Kung, *Proc. 9th Brazilian Congress on Catalysis*, **2**, 498 (1997).
48. "Supported VPO Catalysts for Selective Oxidation of Butane. III Effect of Preparation Procedure and SiO<sub>2</sub> Support," J.M.C. Bueno, G.K. Bethke, M.C. Kung, and H.H. Kung, *Catalysis Today* **43**, 101 (1998).
49. "NO Decomposition on Na-Promoted Co<sub>3</sub>O<sub>4</sub> Catalysts," P. Park, J.-K. Kil, H.H. Kung, and M.C. Kung, *Catalysis Today* **42**, 57 (1998).
50. "Effect of Pt Dispersion on the Reduction of NO by Propene over Alumina-Supported Pt Catalysts under Lean-burn Conditions," J.-H. Lee and H.H. Kung, *Catal. Lett.* **51**, 1 (1998).
51. "Synergistic Effect in Lean NO<sub>x</sub> Reduction by CH<sub>4</sub> over Co/Al<sub>2</sub>O<sub>3</sub> and H-Zeolite Catalysts," J.-Y. Yan, H.H. Kung, W.M.H. Sachtler, and M.C. Kung, *J. Catal.*, **175**, 294 (1998).
52. "Lean NO<sub>x</sub> Catalysis over Sn/γ-Al<sub>2</sub>O<sub>3</sub> Catalysts," M.C. Kung, P.W. Park, D.-W. Kim, and H.H. Kung, *J. Catal.*, **181**, 1 (1999).
53. "Catalytic NO<sub>x</sub> Reduction with Hydrocarbon over Alumina-Supported Catalysts," M.C. Kung, H.H. Kung, K.A. Bethke, J.-Y. Yan, and P.W. Park, *Fundamental and Applied Aspects of Chemically Modified Surfaces*, Ed. J.P. Blitz and C.B. Little, Royal Society of Chemistry, (Proc. 7<sup>th</sup> Intern. Symp. On Chemically Modified Surfaces), 1999, p. 246.
54. "Characterization of SnO<sub>2</sub>/Al<sub>2</sub>O<sub>3</sub> Lean NO<sub>x</sub> Catalysts," P.W. Park, H.H. Kung, D.-W. Kim, and M.C. Kung, *J. Catal.* **184** (1999) 440.

## References

- <sup>1</sup> M.A. Char, D. Patel, M.C. Kung, and H.H. Kung, *J. Catal.*, **105**, 483 (1987).

- 
- 2 H.H. Kung, and M.A. Chaar, U.S. patent 4772319 (1988).
  - 3 M.A. Chaar, D. Patel, and H.H. Kung, *J. Catal.*, **109**, 463 (1988).
  - 4 D. Patel, M.C. Kung, and H.H. Kung, *Proc. 9th Intern. Congr. Catal.*, **4**, 1554 (1988).
  - 5 M.C. Kung, and H.H. Kung, *J. Catal.*, **128**, 287 (1991).
  - 6 H. H. Kung, *Adv. Catal.*, **40**, 1 (1994).
  - 7 D. Patel, P. J. Andersen, and H. Kung, *J. Catal.*, **125**, 130 (1990).
  - 8 Ozie S. Owen and Harold H. Kung, *J. Molec. Catal.*, **79**, 265 (1993).
  - 9 L. Owens, and H.H. Kung, *J. Catal.*, **144**, 202 (1993).
  - 10 P.J. Andersen, and H.H. Kung, *J. Phys. Chem.*, **96**, 3114 (1992).
  - 11 P.M. Michalakos, M.C. Kung, I. Jahan, and H.H. Kung, *J. Catal.*, **140**, 226 (1993).
  - 12 L. Owens, and H.H. Kung, *J. Catal.* **148**, 587 (1994).
  - 13 M.C. Kung, and H.H. Kung, *J. Catal.*, **134**, 668 (1992).
  - 14 S. Sato, Y. Yu-u, H. Yahiro, N. Mizuno, M. Iwamoto, *Appl. Catal.* 70 (1991) L1.
  - 15 W. Held, A. Konig, T. Richtler, L. Ruppe, SAE paper No. 990496, 1990.
  - 16 M. Iwamoto, N. Mizuno, and H. Yahiro, *Proc. 10th Intern. Congr. Catal.*, L. Guzzi, F. Solymosi, and P. Tétényi ed., *Akadémiai Kiadó, Budapest*, 1993, p. 1285.
  - 17 K.A. Bethke and H.H. Kung, *J. Catal.* **172**, 93 (1997).
  - 18 M.C. Kung, H.H. Kung, K.A. Bethke, J.-Y. Yan, and P.W. Park, *Fundamental and Applied Aspects of Chemically Modified Surfaces*, Ed. J.P. Blitz and C.B. Little, Royal Society of Chemistry, (*Proc. 7th Intern. Symp. On Chemically Modified Surfaces*), 1999, p. 246.
  - 19 A. Obuchi, M. Nakamura, A. Ogata, K. Mizuno, A. Ohi, and H. Ohuchi, *J. Chem. Soc. Chem. Commun.* 1992, 1150.
  - 20 E.g. K. Shimizu, H. Kawabata, A. Satsuma, and T. Hattori, *J. Phys. Chem. B* **103**, 5240 (1999).
  - 21 H. Hamada, Y. Kintaichi, T. Yoshinari, M. Tabata, M. Sasaki, and T. Ito, *Catal. Today* **17**, 111 (1993).
  - 22 S.. Masters and D. Chadwick, *Appl. Catal. B: Environmental* **23**, 235 (1999)
  - 23 F.C. Munier, J.P. Breen, and J.R.H. Ross, *Chem. Commun.* 259 (1999).
  - 24 M.C. Kung, J.-H. Lee, A. Chu-Kung, and H.H. Kung, *Proc. 11th Intern. Cong. Catal.* 1996, p. 701.
  - 25 A. Ueda, T. Oshima, and M. Haruta, *Appl Catal. B, Environmental* **12**, 81 (1997).
  - 26 T. Miyadera, *Appl. Catal. B: Environmental* **2**, 199 (1993).
  - 27 Y. Li and J.N. Armor, *Appl. Catal. B: Environmental* **1**, L31 (1992).
  - 28 J.Y. Yan, M.C. Kung, W.M.H. Sachtler, and H.H. Kung, *J. Catal.* **172**, 178 (1997).
  - 29 M.C. Kung, P.W. Park, D.-W. Kim, and H.H. Kung, *J. Catal.* **181**, 1 (1999).
  - 30 P.W. Park, H.H. Kung, D.-W. Kim, and M.C. Kung, *J. Catal.* **184**, 440 (1999).
  - 31 R. Burch, P. Fornasiero, B.W.L. Southward, *J. Catal.* **182**, 234 (1999).
  - 32 J.-H. Lee and H.H. Kung, *Catal. Lett.* **51**, 1 (1998).
  - 33 P. Denton, A. Giroir-Fendler, H. Praliaud, and M. Primet, *J. Catal.* **189**, 410 (2000).
  - 34 A. Yezerets, Y. Zheng, P.W. park, M.C. Kung, and H.H. Kung, *Proc. 12th Intern. Cong. Catal., Stud. Surf. Sci. Catal.* **130**, 629 (2000).
  - 35 Inaba, M., Kintaichi, Y. And Hamada, H., *Catal. Lett.* **36**, 223 (1996).